INSTITUTE OF PHYSICS PUBLISHING SUPERCONDUCTOR SCIENCE AND TECHNOLOGY

Supercond. Sci. Technol. **16** (2003) 183–187 PII: S0953-2048(03)54973-9

Vortex dynamics and pinning properties analysis of MgB_2 bulk samples by ac susceptibility measurements

C Senatore[1], M Polichetti[1], D Zola[1], T Di Matteo[1], G Giunchi[2] and S Pace[1]

[1] Dipartimento di Fisica 'E R Caianiello' and INFM, Università di Salerno, Baronissi, Italy
[2] EDISON S.p.A., Milano, Italy

E-mail: carmelo@sa.infn.it(C Senatore)

Received 16 October 2002
Published 30 December 2002
Online at stacks.iop.org/SUST/16/183

Abstract

Flux line dynamics have been investigated on MgB_2 bulk superconductors obtained by reactive liquid infiltration by measuring the ac magnetic susceptibility. The fundamental and third harmonics have been studied as a function of temperature, dc magnetic field, ac field amplitude and frequency. In order to determine the dynamical regimes governing the vortex motion, the experimental results have been compared with susceptibility curves obtained by numerical calculations of the non-linear diffusion equation for the magnetic field. The frequency behaviour of the third harmonic response, that cannot be explained by frequency dependent critical state models, has been related to the current dependence of the flux creep activation energy $U(J)$ in the diffusion coefficient. In this way we have shown that the measured curves are correctly interpreted within the framework of a vortex glass description.

1. Introduction

The discovery of superconductivity in MgB_2 with a transition temperature near to 39 K has led to considerable interest in this binary compound, since there are many proposals for its potential uses exploiting its intrinsic properties. However, the low value of the irreversibility field and the rapid decrease of the critical current density J_c with the magnetic field [1] actually represent a limitation for the high field power applications of MgB_2. Many attempts to improve the transport properties by way of proton irradiation [2], alloying and nanoparticle additions [1, 3, 4] have been made but the results, although promising, are still not conclusive. However, to overcome the present limits of this compound it is necessary to fully understand its pinning properties.

One of the most popular means of investigating the vortex dynamics as well as the pinning properties in type-II superconductors is the measurement of the response of the vortex lattice to ac magnetic fields [5]. The ac susceptibility represents a powerful tool to study the different dynamical regimes of the flux lines: this technique allows changes to be induced in the vortex dynamic by changing the value of the external parameters, such as the ac field frequency and amplitude, the dc field intensity, the temperature, etc. Moreover, in addition to the first harmonic response, the higher order harmonics of ac susceptibility can provide much insight into the loss mechanisms and the flux motion. In fact the response of type-II superconductors to an ac magnetic field can be either linear or non-linear. The linear response can be divided into two different frequency regimes. At high frequency, the response is dominated by a viscous motion of the vortex liquid (flux flow regime) [6]. In the region of extremely low frequency, thermally activated vortex jumps between most favourable metastable states of the vortex lattice come into play (TAFF regime) [7] and contribute to the ac response, especially near T_c. In both these cases the linear response results from an Ohmic resistive state $E = \rho J$ in the sample, where $\rho(B, T)$ is independent of J. Therefore, in the presence of a dc field larger than the ac one, the electrodynamics of a superconductor in these regimes can be described in terms of a normal metal, governed by the skin effect. In contrast, at intermediate frequencies, when the

vortex motion is governed by relevant thermally activated flux creep phenomena, the resistivity of the sample is expressed by the J-dependent thermally activated form:

$$\rho(J) = \rho_0 \exp\left[-\frac{U(J)}{k_B T}\right] \tag{1}$$

with $U(J)$ the effective activation energy. The non-linear behaviour, exhibited in these conditions by the E–J characteristic, as a consequence of the current dependence of the pinning energy, leads to higher harmonic generation in the ac susceptibility. Moreover, the non-linearity and, therefore, the anharmonicity of the response change with the electrical field induced in the sample by changing the frequency of the ac magnetic field. The aim of this work is to investigate the relation between the frequency behaviour of the third harmonic response of ac susceptibility χ_3 and the dependence of the activation energy $U(J)$ on the current density in order to individuate the dynamical regimes governing the vortex motion. In order to do this, we have compared the experimental $\chi_3(T)$ curves measured for MgB_2 bulk superconductors with the simulated behaviour obtained by the numerical integration of the magnetic field diffusion equation for different functional forms of $U(J)$.

This paper is organized as follows. In section 2 we report the numerical method applied to resolve the flux diffusion equation. The fundamental and third harmonic measurements performed on MgB_2 bulk samples have been discussed and compared with the calculated curves in section 3. Finally, section 4 is dedicated to a summary of this work.

2. Numerical method

Since the harmonic susceptibilities are determined by the magnetic flux entering and leaving the sample, we need to study the non-linear diffusion-like equation that governs the spatial–temporal evolution of the local magnetic field in a superconductor. In the case of an infinite slab of thickness d in a parallel field geometry this equation can be written as [8]:

$$\frac{\partial B}{\partial t} = \frac{\partial}{\partial x}\left[\frac{\rho(B, T, J)}{\mu_0}\frac{\partial B}{\partial x}\right] \tag{2}$$

where $\rho(B, T, J)$ is the residual resistivity due to the flux motion. The proper boundary conditions are $B(\pm d/2, t) = B_{\rm ext}(t) = B_{\rm dc} + B_{\rm ac}\sin(2\pi f t)$.

Equation (2) has been numerically solved by means of the Fortran NAG [9] routines. The algorithm computes the time evolution of the local field profile by integrating a discrete version of equation (2) using Gear's method for a fixed number of spatial meshes. In order to obtain the harmonic susceptibilities $\chi_n = \chi_n' + {\rm i}\chi_n''$, first we have calculated the magnetization M for the applied time-dependent field, i.e. the magnetization loop, and then its Fourier transforms.

The diffusion coefficient $\rho(B, T, J)/\mu_0$ is related to the thermally activated flux motion, leading to electric fields of the form:

$$E = \rho_n \frac{B}{B_{c2}(T)} J_c(B, T) \exp\left[-\frac{U_P(B, T, J)}{k_B T}\right]. \tag{3}$$

We assume that the temperature, magnetic field and current density dependence in the effective energy barrier $U_P(B, T, J)$ may be separated [10] by using, for the current dependence, the general form [11]

$$U(J) = \frac{U_0}{\mu}\left[\left(\frac{J_c}{J}\right)^{\mu} - 1\right]. \tag{4}$$

Using this general expression, different dynamic behaviour, related to the current dependence of the activation energy, can be analysed. In particular, the choice $\mu = -1$ corresponds to the usual Kim–Anderson (KA) model [12]. On the other hand, the flux creep phenomena in the case of collective pinning by weak disorder, corresponding to a vortex glass state, can be recovered from (4) by imposing $0 < \mu < 1$ [13]. Depending on the density of impurities, in a type-II superconductor two types of vortex glass states could exist. The first one is the strongly disordered vortex glass phase as described by Fisher *et al* [14]. The second one is the quasi-ordered Bragg glass established by Giamarchi and Le Doussal [15, 16]. However, both these two glassy states of the flux lines lead, for the $U(J)$ dependence, to a power law with $0 < \mu < 1$. Although experimentally μ has been found to depend on both temperature and field [17], in the VG model it is regarded as a universal exponent with a single value, and moreover the choice $\mu = {\rm const}$ correctly describes the measured data for a wide range of current densities [18, 19]. For this reason, we performed our calculation by considering different constant values of $\mu = 0.1, 0.2, 0.5, 0.8$ and -1, thus both in the VG and KA picture. In particular, in the framework of the VG approach for brevity we report here only the curves calculated for the value of the exponent $\mu = 0.5$.

In order to take into account the temperature dependence of the ac susceptibilities, we have to specify the temperature dependences of the critical current density $J_c(T)$ and the activation energy $U_P(T)$. For this purpose, we have adopted the expressions predicted by the collective pinning (CP) model [7, 20]:

$$\begin{aligned} U_P(T) &= U_0[1 - (T/T_c)^4] \\ J_c(T) &= J_0[1 - (T/T_c)^2]^{5/2}[1 + (T/T_c)^2]^{-1/2}. \end{aligned} \tag{5}$$

Since the simulated curves reported in this paper have been calculated for $B_{\rm dc} \gg B_{\rm ac}$ ($B_{\rm ac} = 4$ G, $B_{\rm dc} = 200$ G), we have neglected the dependence of both J_c and U_0 on the ac magnetic field.

The upper critical field has been written as $B_{c2}(T) = B_{c2}(0)[1 - (T/T_c)^2]/[1 + (T/T_c)^2]$ [21]. The material parameters used for all calculations presented in this work pertain to an MgB_2 slab of thickness $d = 0.5$ mm, $T_c = 38.8$ K, $B_{c2}(0) = 15$ T, $U_0(B_{\rm dc} = 200\ {\rm G})/k_B = 8000$ K, $J_0(B_{\rm dc} = 200\ {\rm G}) = 5 \times 10^8$ A m^{-1}, $\rho_n = 2 \times 10^{-5}\ \Omega$ m.

3. Experimental results and discussion

We performed our ac susceptibility studies on highly dense ($\rho = 2.4$ g cm^{-3}) polycrystalline MgB_2 bulk samples prepared by reactive liquid infiltration [22]. Due to this high density, the intrinsic granularity of the samples does not affect the supercurrent flow and then the magnetic behaviour of the material. The temperature dependences of both the first and the third harmonics have been measured by changing the temperature with a rate $\Delta T/\Delta t = 0.4$ K min^{-1} from 4.2 K to 45 K, using different ac field amplitudes (1, 4, 8, 16 G) in the frequency range 27–3507 Hz, with a dc field $B_{\rm dc}$ ranging

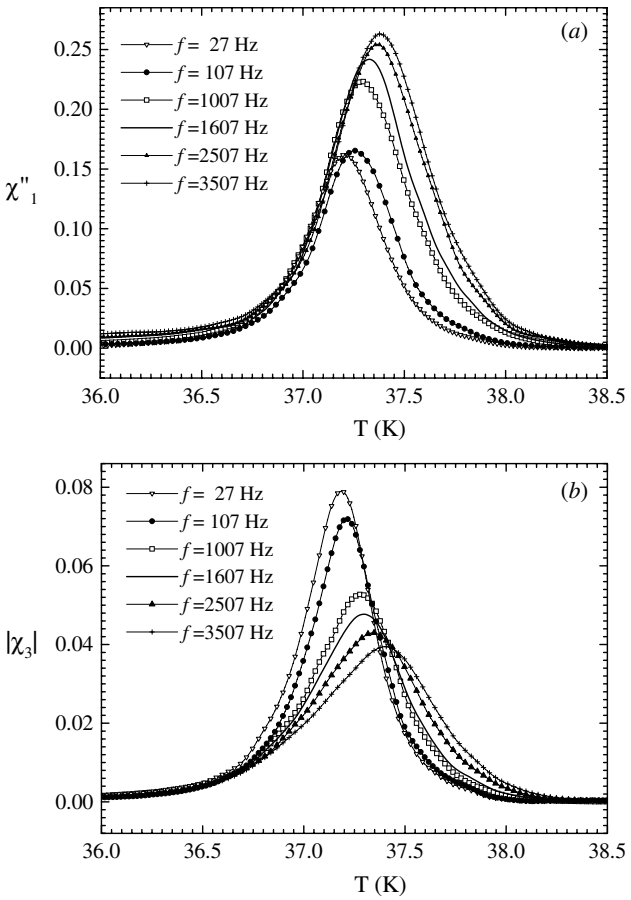

Figure 1. Temperature dependence of χ_1'' (*a*) and $|\chi_3|$ (*b*) measured at $B_{ac} = 4$ G and $f = 27$, 107, 1007, 1607, 2507, 3507 Hz in zero dc field.

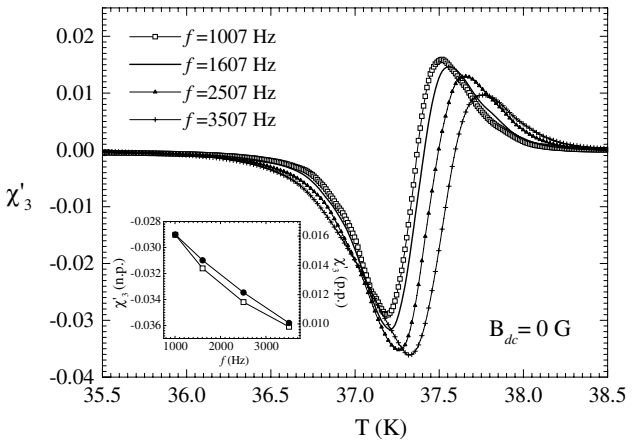

Figure 2. Temperature dependence of χ_3' curves measured at $B_{ac} = 4$ G and $f = 1007$, 1607, 2507, 3507 Hz in zero dc field. Inset: frequency behaviour of the negative peak (open squares) and the positive peak (solid circles) for the measured χ_3' curves.

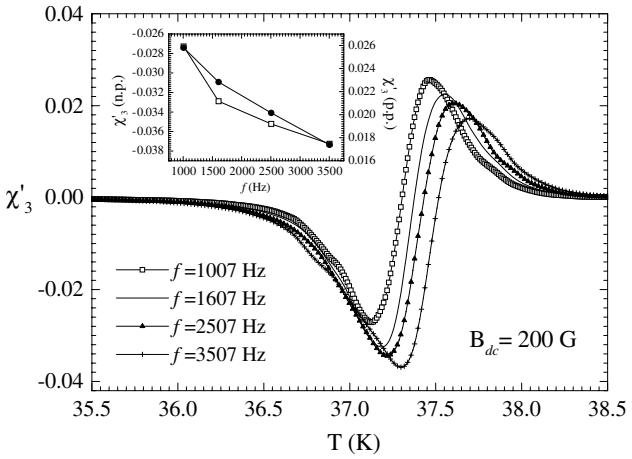

Figure 3. Temperature dependence of χ_3' curves measured at $B_{ac} = 4$ G, $B_{dc} = 200$ G and $f = 1007$, 1607, 2507, 3507 Hz. Inset: frequency behaviour of the negative peak (open squares) and the positive peak (solid circles) for the measured χ_3' curves.

from 0 to 200 G. The measurements reported in this paper have been performed on a sample whose dimensions are $20 \times 2.9 \times 0.4$ mm^3. Both the ac and the dc field are applied parallel to the length of the sample. It exhibits quite a sharp transition with $T_c = 38.8$ K, evaluated by the real part of χ_1 measured for $B_{ac} = 1$ G and $f = 3507$ Hz; the transition width, estimated by the 10–90% criterion, is about 1 K.

The measured $\chi_1''(T)$ curves reported in figure 1(*a*) show the increase of both the temperature and the amplitude of the peak with the frequency. Also in the $|\chi_3|(T)$ measurements (figure 1(*b*)) a pronounced frequency dependence appears. In fact, by increasing the frequency not only the position of the peak moves toward higher temperatures, but also its height decreases.

Since the experimental data show clear frequency dependences, a simple critical state description [23] is not suitable. Indeed, in the framework of the Bean model, the harmonic susceptibilities can be reduced to universal curves that describe the ac response of a hard superconductor as a function of a single parameter δ, which is the ratio between the full penetration field and the amplitude of the applied alternating field [24]. Therefore, although the introduction of a frequency dependent critical current density might explain the temperature shift of the peak of the harmonic susceptibilities, which is due to the increase in the current induced by a higher ac field frequency, the same model is not suitable to explain the change in the peak heights which, in this picture, have a defined and constant value.

In contrast, considering the presence of vortex dynamical regimes and by numerically integrating the magnetic diffusion equation, it has been shown that the increase of the amplitude of $\chi_1''(T_P)$ with the frequency is an indication of the reduction of the non-linear behaviour of the *I–V* characteristic driven by the increased electric field [25]. However, to investigate the flux dynamic in more detail we have focused our analysis on the third harmonic components, due to their higher sensitivity to the changes in the dynamical regimes. In particular, the comparison between the experimental $\chi_3'(T)$ curves, reported in figures 2 and 3, and the simulated ones in [26], indicates that the vortex dynamic in the analysed sample is dominated by the flux creep phenomena, at least in the frequency range of our measurements. From the measurements at increasing frequencies it is clear that the ratio between the heights of the $\chi_3'(T)$ peaks (the positive one and the negative one), in absolute value, changes. From the comparison of figures 2 and 3, where we show the measured $\chi_3'(T)$ curves for $B_{dc} = 0$ G and $B_{dc} = 200$ G, respectively,

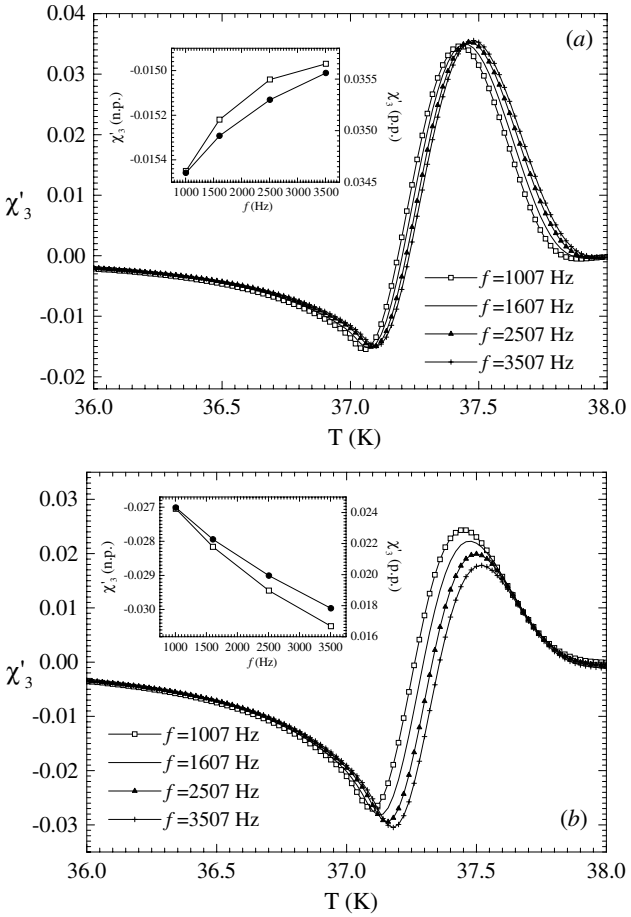

Figure 4. Temperature dependence of χ'_3 curves calculated for $B_{ac} = 4$ G, $B_{dc} = 200$ G and $f = 1007$, 1607, 2507, 3507 Hz by using (*a*) the KA $U(J)$ dependence, (*b*) a VG-type $U(J)$ dependence in the diffusion coefficient. Insets: frequency behaviour of the negative peak (open squares) and the positive peak (solid circles) for the calculated χ'_3 curves.

we have the result that a non-zero dc magnetic field does not affect the frequency behaviour of the $\chi'_3(T)$ peaks but just modifies their height. In terms of the model reported in section 2, a non-zero dc field $B_{dc} \gg B_{ac}$ emphasizes the non-linearity related to the J-dependence in $\rho(B, T, J)/\mu_0$, making the harmonic contribution due to the B/B_{c2} term in the diffusion coefficient (3) negligible. Moreover, our numerical calculations show that in the KA scenario the height of the positive and negative peaks increases (figure 4(*a*)) with the frequency, whereas in the VG approach the height of both the peaks decreases (figure 4(*b*)). In this way, the frequency dependence of the $\chi'_3(T)$ curves can provide a valid criterion to distinguish the current dependence form of the activation energy $U(J)$ in the sample. The comparison between the experiments and the simulations shows that the behaviour encountered in the VG approach is the one which agrees better with the frequency dependence of the measured $\chi'_3(T)$ curves, as is visible in figure 3 for the particular values $B_{ac} = 4$ G and $B_{dc} = 200$ G. However, it can be noted that the decrease of the peak height is weaker in the simulated curves than in the measured ones. This could be ascribed to the values assumed for the parameters in the numerical calculations. We have also verified, by means of simulations performed for other values of μ, that the frequency behaviour of the $\chi'_3(T)$ peaks is not affected by the particular choice of $\mu \in (0, 1)$. The only variations in the curves calculated for different values of the exponent μ are with regard to the transition width and the ratio between the heights of the positive and negative peaks. In support of the agreement between the simulations and the experiment, it can be noted that the decrease of $|\chi_3|(T)$ for increasing frequencies, reported in figure 1(*b*), and the reduction of the non-linearity, evidenced from the $\chi''_1(T)$ curves in figure 1(*a*), are also predicted by the numerical simulations in the VG approach [27]. Our analysis is also confirmed by the measurements of the fundamental and third harmonic performed with $B_{ac} = 1$, 8, 16 G and not reported here for brevity. Therefore, our results indicate that the experimental ac magnetic response of our MgB_2 samples is governed by a vortex glass dynamic regime, likely due to the presence of quenched random point-size disorder [22] which promotes the highly disordered glass phase in the vortex matter, as already reported in the literature for this kind of material [28].

4. Conclusions

In this paper, we have analysed the frequency dependence of the ac susceptibilities χ_1 and χ_3 on MgB_2 bulk samples, prepared by reactive liquid infiltration. In particular, by comparison with the numerical calculations of the flux diffusion equation, we have shown that our experimental results represent a strong indication about the presence of a vortex glass dynamic governing the ac magnetic response of the samples.

Acknowledgments

We want to thank Mr L Falco and Mr A Ferrentino for their technical support.

References

[1] Buzea C and Yamashita T 2001 *Supercond. Sci. Technol.* **14** 115
[2] Bugoslavsky Y, Cohen L F, Perkins G K, Polichetti M, Tate T J, William R G and Caplin A D 2001 *Nature* **411** 561
[3] Toulemonde P, Musolino N and Flükiger R 2002 *Preprint* cond-mat/0207033
[4] Wang J *et al* 2002 *Preprint* cond-mat/0207080
[5] Gömöry F 1997 *Supercond. Sci. Technol.* **10** 523
[6] Bardeen J and Stephen M J 1965 *Phys. Rev.* A **140** 1197
[7] Blatter G *et al* 1994 *Rev. Mod. Phys.* **66** 1125
[8] van der Beek C J, Geshkenbein V B and Vinokur V M 1993 *Phys. Rev.* B **48** 3393
[9] NAG Fortran Library 1991 *Revised Version 15 User Manual*
[10] Perkins G K and Caplin A D 1996 *Phys. Rev.* B **54** 12551
[11] Qin M J and Ong C K 1999 *Physica* C **319** 41
[12] Anderson P W and Kim Y B 1964 *Rev. Mod. Phys.* **36** 39
[13] Feigel'man M V *et al* 1989 *Phys. Rev. Lett.* **63** 2303
[14] Fisher D S, Fisher M P A and Huse D A 1991 *Phys. Rev.* B **43** 130
[15] Giamarchi T and Le Doussal P 1994 *Phys. Rev. Lett.* **72** 1530
[16] Giamarchi T and Le Doussal P 1995 *Phys. Rev.* B **52** 1242
[17] Sun Y R *et al* 1993 *Phys. Rev.* B **47** 14481
[18] Ji H L *et al* 1994 *J. Appl. Phys.* **75** 1671
[19] Rui Y *et al* 1995 *Phys. Rev.* B **51** 9161

[20] Hagen C W and Griessen R 1989 *Phys. Rev. Lett.* **62** 2857
[21] Coffey M W and Clem J R 1992 *Phys. Rev.* B **45** 9872
[22] Giunchi G *et al* 2002 *Int. J. Mod. Phys.* to be published (*Preprint* cond-mat/0208040)
[23] Bean C P 1964 *Rev. Mod. Phys.* **2** 31
[24] Shatz S, Shaulov A and Yeshurun Y 1993 *Phys. Rev.* B **48** 13871
[25] Di Gioacchino D, Celani F, Tripodi P, Testa A M and Pace S 1999 *Phys. Rev.* B **59** 11539
[26] Qin M J and Ong C K 1999 *Physica* C **319** 41
[27] Di Gioacchino D, Tripodi P, Celani F, Testa A M and Pace S 2001 *IEEE Trans. Appl. Supercond.* **11** 3924
[28] Angst M *et al* 2002 *Phys. Rev.* B to be published (*Preprint* cond-mat/0205293)